phosphorus atom.[1] A high $^1J(^{195}\mathrm{Pt},\mathrm{P}_2)$ value corresponds to a small trans influence, which is represented in that case by the platinum 6s character of the Pt–L bond increasing at the expense of the trans Pt–P bond that is in competition for the same s ± d hybrid orbital.[8] The two trans influence orders obtained from the $\Delta(\mathrm{P}_2)$ and $^1J(^{195}\mathrm{Pt},\mathrm{P}_2)$ parameters, respectively, are $\mathrm{SnCl_3^-} \sim \mathrm{H^-} > \mathrm{P(OMe)_3} \sim \mathrm{SCN^-} \sim \mathrm{P\ (OEt)_3} > \mathrm{Cl^-} \sim \mathrm{PEt_3} > \mathrm{NCS^-}$ and $\mathrm{H^-} > \mathrm{P(OEt)_3} \sim \mathrm{P(OMe)_3} \sim \mathrm{PEt_3} > \mathrm{SnCl_3^-} > \mathrm{SCN^-} > \mathrm{Cl^-} \sim \mathrm{NCS^-}$.

At first glance the two series look different. However, both series have common trends that are in agreement with previously published trans influence series.[1,2,8] The position of the hydride in front of the two series is characteristic for the strong Pt–H interaction found in platinum(II) hydrides.[8] Typically phosphites exert a stronger trans influence than phosphines do.[1,8] The same is true for S-bonded versus N-bonded thiocyanate, and the position of chloride and N-bonded species at the end of the series is characteristic, too.

Acknowledgment. This work was supported by the Land Vorarlberg, Austria.

Registry No. 1a, 110795-97-6; **1b**, 110795-98-7; **2**, 110795-99-8; $[\mathrm{PtCl(PP_3)}]\mathrm{Cl}$, 104845-13-8; $[\mathrm{Pt(NCS)(PP_3)}]\mathrm{BF_4}$, 110796-01-5; $[\mathrm{Pt(SCN)(PP_3)}]\mathrm{BF_4}$, 110796-03-7; $\mathrm{K_2PtCl_4}$, 10025-99-7.

Contribution from the Department of Chemistry
and Laboratory for Molecular Structure and Bonding,
Texas A&M University, College Station, Texas 77843

Reactions of $\mathrm{Rh_2(O_2CCH_3)_2(C_6H_4PPh_2)_2{\cdot}2CH_3COOH}$ with Chlorotrimethylsilane in the Presence of Monodentate Phosphines To Give $[\mathrm{Rh_2Cl_2(C_6H_4PPh_2)_2(PPh_3)_2}]$ and $[\mathrm{Rh_2Cl_2(C_6H_4PPh_2)_2(PMe_3)_2}]$

F. Albert Cotton,* Kim R. Dunbar, and Cassandra T. Eagle

Received June 10, 1987

One of our recent interests in this laboratory has been to extend the chemistry of the $\mathrm{Rh_2^{4+}}$ unit in new directions.[1] We have found that a powerful method for doing this is to employ $\mathrm{Me_3SiCl}$ as a reagent for replacing $\mathrm{MeCO_2^-}$ ligands by $\mathrm{Cl^-}$ ligands, while simultaneously providing phosphine ligands to complete the coordination sphere. When $\mathrm{Rh_2(O_2CMe)_4}$ was reacted with 2 equiv of $\mathrm{Me_3SiCl}$ and dppm ($\mathrm{Ph_2PCH_2PPh_2}$) or $\mathrm{Rh_2(O_2CMe)_2(C_6H_4PPh_2)_2}$ with 2 $\mathrm{Me_3SiCl}$ and dmpm ($\mathrm{Me_2PCH_2PMe_2}$), products with four bridging ligands and two axial Cl ligands, viz., $\mathrm{Rh_2(O_2CMe)_2(dppm)_2Cl_2}$[1b] and $\mathrm{Rh_2(C_6H_4PPh_2)_2(dmpm)_2Cl_2}$,[1] were isolated and characterized. These results are chemically and structurally quite reasonable and were not considered surprising.

After the preparation of $\mathrm{Rh_2(O_2CMe)_2(dppm)_2Cl_2}$ had been accomplished by using 2 equiv of $\mathrm{Me_3SiCl}$ to replace two $\mathrm{MeCO_2^-}$ ligands from $\mathrm{Rh_2(O_2CMe)_4}$, a similar reaction employing 4 equiv was carried out with the goal of obtaining a product of type I, or possibly II. A product of this stoichiometry was in fact obtained, but its structure was different from either of those anticipated, namely of type III.[1b] The explanation presented for this is that a structure of type III permits all of the metal–ligand bonds present in I or II to be retained, including the Rh–Rh single bond, while also allowing the formation of two more Rh–Cl bonds when two Cl atoms become bridging instead of terminal.

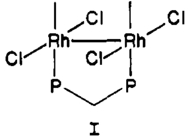

I

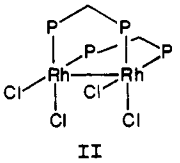

II

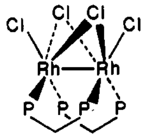

III

To pursue this type of chemistry further, we have now examined some similar reactions, but with the use of monophosphines rather than the potentially bridging diphosphinomethanes. The results of these studies are reported here.

Experimental Section

The starting materials, $\mathrm{Rh_2(O_2CCH_3)_4}$[2] and $\mathrm{Rh_2(O_2CCH_3)_2C_6H_4PPh_2{\cdot}2CH_3COOH}$,[3] were prepared according to published procedures. Chlorotrimethylsilane ($\mathrm{Me_3SiCl}$) was obtained from Aldrich Chemical Co. and used without further purification. Triphenylphosphine ($\mathrm{PPh_3}$) and trimethylphosphine ($\mathrm{PMe_3}$) were purchased from Strem Chemicals. $\mathrm{PPh_3}$ was recrystallized from ethanol; $\mathrm{PMe_3}$ was used as received. All solvents were dried and freshly distilled under dinitrogen prior to use.

Complexes **1** and **2** were prepared under an argon atmosphere by the same general route. $\mathrm{Rh_2(O_2CCH_3)_2(C_6H_4PPh_2)_2{\cdot}2CH_3COOH}$ (0.150 g, 0.155 mmol) was dissolved in 15 mL of THF. The solution was warmed to 60 °C and $\mathrm{Me_3SiCl}$ (80 μL, 4 equiv) was injected into the reaction vessel. The reaction mixture was then treated with 2.1 equiv of the appropriate phosphine. The solutions were refluxed for 30 min, cooled to room temperature, and then concentrated under vacuum to ca. 5 mL. The precipitated products were washed with three 5-mL portions of $\mathrm{Et_2O}$ and dried under vacuum. Complex **1** was recrystallized from $\mathrm{CHCl_3}$ solution by introducing an upper layer of $\mathrm{Et_2O}$. A higher yield of crystalline material was formed when a trace quantity of $\mathrm{PPh_3}$ was added to the $\mathrm{CHCl_3}$ solution (yield 0.168 g, 82%). IR (Nujol mull, CsI): 1585 (w), 1575 (w), 1560 (m), 1540 (w), 1483 (s), 1435 (s), 1415 (m), 1320 (w), 1240 (m), 1190 (w), 1160 (w), 1120 (w), 1090 (s), 1075 (w), 1030 (w), 1005 (w), 750 (s), 730 (s), 720 (w), 700 (s), 625 (w), 550 (s), 500 (m), 490 (m), 465 (m), 420 (w) $\mathrm{cm^{-1}}$. Complex **2** was recrystallized from a mixture of THF and toluene that was carefully layered with a mixture of $\mathrm{Et_2O}$ and hexane. In contrast to the case for **1**, **2** crystallized more readily in the absence of excess monodentate ligand (yield 0.112 g, 76%). IR (Nujol mull, CsI): 1582 (w), 1565 (m), 1542 (m), 1435 (m), 1410 (m), 1300 (m), 1285 (m), 1235 (w), 1185 (w), 1170 (w), 1115 (w), 1095 (m), 1090 (m), 1075 (w), 1030 (w), 1015 (m), 1005 (w), 900 (s), 845 (m), 745 (s), 735 (s), 715 (s), 675 (w), 650 (w), 545 (s), 530 (w), 505 (s), 485 (m), 445 (w), 430 (w) $\mathrm{cm^{-1}}$.

X-ray Crystallography. The structures of **1** and **2** were determined by general procedures that have been fully described elsewhere.[4] Data reductions were carried out by standard methods using well-established computational procedures.[5] The crystal parameters and basic information pertaining to data collection and structure refinement are summarized in Table I. Tables II and III list the positional parameters for structures **1** and **2**, respectively. Selected bond distances and angles of **1** and **2** are found in Tables IV and V, respectively. Complete tables of bond distances and angles as well as anisotropic thermal parameters and structure factors are available as supplementary material.

$\mathbf{Rh_2Cl_2(C_6H_4PPh_2)_2(PPh_3)_2}$ **(1).** A bright red prism of **1** was mounted on a glass fiber. A rotation photograph indicated that the crystal diffracted well. An automatic search routine was used to locate 25 high-angle reflections. The reduced cell dimensions indicated that the crystal belonged to the monoclinic crystal system, which was verified by axial photography. Systematic absences led to the choice of two possible space groups, *C*2/*c* and *Cc*. The former was found to be correct on the basis of successful refinement. The ω–2θ scan motion was used to gather 5582 possible data points in the range $4 < 2\theta < 50°$. Three standard reflections measured following every 150 scans did not significantly change in intensity over the 22 h of beam exposure, and no decay correction was applied. Azimuthal scans of six reflections with Eulerian angle χ near

---

(1) (a) Cotton, F. A.; Dunbar, K. R. *J. Am. Chem. Soc.* **1987**, *109*, 3142. (b) Cotton, F. A.; Dunbar, K. R.; Verbruggen, M. *J. Am. Chem. Soc.* **1987**, *109*, 5498.

(2) Rempel, G. A.; Legzdins, P.; Smith, H.; Wilkinson, G. *Inorg. Synth.* **1972**, *13*, 90.

(3) Chakravarty, A. R.; Cotton, F. A.; Tocher, D. A.; Tocher, J. H. *Organometallics* **1985**, *4*, 8.

(4) (a) Bino, A.; Cotton, F. A.; Fanwick, P. E. *Inorg. Chem.* **1979**, *18*, 3558. (b) Cotton, F. A.; Frenz, B. A.; Deganello, G.; Shaver, A. *J. Organomet. Chem.* **1973**, *50*, 227.

(5) Crystallographic computing was done on a MicroVAX computer (MicroVMS V4.5).

Table I. Crystallographic Data for $Rh_2Cl_2(Ph_2P\{C_6H_4\})_2(PPh_3)_2$ and $Rh_2Cl_2(Ph_2P\{C_6H_4\})_2(PMe_3)_2 \cdot C_7H_8 \cdot OC_4H_8$

formula	$Rh_2Cl_2P_4C_{72}H_{58}$	$Rh_2Cl_2P_4OC_{53}H_{62}$
fw	1323.88	1115.65
space group	*C*2/*c*	*Pbcn*
systematic absences	hkl, $h + k \neq 2n$; $h0l$, $l \neq 2$n	$0kl$, $k \neq 2n$; $h0l$, $l \neq 2n$; $hk0$, $h + k \neq 2n$
a, Å	26.257 (4)	22.059 (5)
b, Å	14.085 (2)	18.949 (5)
c, Å	17.315 (3)	22.450 (6)
β, deg	113.2 (2)	
V, Å^3	5885 (3)	9384 (4)
Z	4	8
d_{calcd}, g/cm^3	1.494	1.557
cryst size, mm	0.25 × 0.20 × 0.30	0.50 × 0.50 × 0.30
μ(Mo Kα), cm^{-1}	7.932	9.793
data collcn instrum	Rigaku AFC5R	Syntex P3
radiation (monochromated in incident beam)	Mo Kα ($\lambda_{\bar{a}}$ = 0.71073 Å)	
orientation reeflns: no.; range (2θ), deg	13; 20.1–25.8	25; 26.5–33.1
temp, °C	23	22
scan method	ω–2θ	ω–2θ
data collecn range, 2θ, deg	$4 < 2\theta < 50$	$4 < 2\theta < 45$
no. of unique data, total with $F_o^2 > 3\sigma(F_o^2)$	5452, 2975	6144, 4461
no. of params refined	361	465
R^a	0.0528	0.0439
R_w^b	0.0704	0.0620
quality-of-fit indicator^c	1.391	1.686
largest shift/esd, final cycle	0.01	0.13
largest peak, e/Å^3	0.329	0.6455

[a] $R = \sum||F_o| - |F_c||/\sum|F_o|$. [b] $R_w = [\sum w(|F_o| - |F_c|)^2/\sum w|F_o|^2]^{1/2}$; $w = 1/\sigma^2(|F_o|)$. [c] Quality of fit = $[\sum w(|F_o| - |F_c|)^2/(N_{observns} - N_{params})]^{1/2}$.

90° were used as the basis for an empirical absorption correction.[6] After the equivalent reflections were averaged, there remained 5452 unique data and 2975 reflections with $F_o^2 \geq 3\sigma(F_o)^2$. At the end of data collection, 13 high-2θ-angle reflections with $2\theta > 20°$ and $F_o > 70$ were used to obtain more accurate cell parameters, which are reported herein.

The direct-methods SHELXS-86 program was used to locate the rhodium atom, which was related by a twofold rotation axis to the second rhodium atom. A sequence of successive difference Fourier maps and least-squares refinement cycles in the VAX SDP package led to the full development of the coordination sphere. Anisotropic refinement was successfully completed with no significant peaks in the final difference Fourier map.

$Rh_2Cl_2(C_6H_4PPh_2)_2(PMe_3)_2$ (2). An orange-red prism-shaped crystal of **2** was mounted on a glass fiber. A rotation photograph indicated that the crystal diffracted well. From the rotation photograph, 17 film coordinates were chosen for a search routine, which refined the coordinates and used them to generate the initial cell parameters. The reduced cell dimensions indicated that the crystal belonged to the orthorhombic crystal system, which was verified by axial photography. Preliminary data collection was performed to locate 25 reflections, which produced more accurate cell parameters. After data collection, 25 reflections with $26.5 < 2\theta < 33.1°$ produced the cell parameters reported in Table I. Systematic absences led to the unique determination of the space group as *Pbcn*. The ω–2θ scan motion was used to collect 6750 possible data points in the range $4 < 2\theta < 45°$. Three standard reflections, measured every 100 scans, did not significantly change in intensity over the 118 h of beam exposure, and no correction for decay was applied. Azimuthal scans of six reflections with Eulerian angle χ near 90° were used as the basis for an empirical absorption correction.[6] After the equivalent reflections were averaged, there were 6144 unique data and 4461 reflections with $F_o^2 \geq 3\sigma(F_o)^2$.

The direct-methods SHELXS-86 program was used to locate the two independent rhodium atoms. A sequence of successive difference Fourier maps and least-squares refinement cycles in the VAX SDP package led to the full development of the coordination sphere. A difference Fourier map revealed peaks due to interstitial solvent molecules. It was discovered that one molecule of toluene and a molecule of THF also belong to the asymmetric unit. The dirhodium molecule was refined anisotropically, but the atoms of the solvent molecules were isotropically refined. In order to refine the parameters of the solvent molecules, the penultimate cycles of the refinement were done in the SHELX-76 package. The data were then transferred back into the VAX SDP package, and a final structure factor calculation was performed.

Table II. Atomic Positional Parameters and Equivalent Isotropic Displacement Parameters (Å^2) and Their Estimated Standard Deviations for $Rh_2Cl_2(Ph_2P\{C_6H_4\})_2(PPh_3)_2$[a]

atom	*x*	*y*	*z*	*B*
Rh	0.45031 (2)	0.18158 (4)	0.24056 (4)	2.40 (1)
Cl	0.52454 (8)	0.0797 (2)	0.3517 (1)	3.27 (5)
P(1)	0.46770 (9)	0.2909 (2)	0.3413 (1)	2.75 (5)
P(2)	0.36503 (8)	0.1026 (2)	0.2213 (1)	2.94 (5)
C(1)	0.5417 (3)	0.3152 (6)	0.3894 (5)	3.1 (2)
C(2)	0.4224 (3)	0.2790 (6)	0.1475 (5)	2.9 (2)
C(3)	0.3672 (3)	0.3078 (6)	0.1130 (5)	3.6 (2)
C(4)	0.3483 (4)	0.3655 (7)	0.0412 (6)	4.5 (2)
C(5)	0.3813 (4)	0.3952 (7)	0.0017 (6)	4.5 (2)
C(6)	0.5629 (4)	0.3698 (7)	0.4626 (5)	3.9 (2)
C(7)	0.4484 (3)	0.2647 (6)	0.4316 (5)	3.1 (2)
C(8)	0.4315 (4)	0.3394 (7)	0.4691 (6)	4.6 (2)
C(9)	0.4147 (4)	0.3173 (9)	0.5376 (6)	5.8 (3)
C(10)	0.4172 (4)	0.2223 (8)	0.5635 (6)	5.2 (3)
C(11)	0.4358 (4)	0.1512 (8)	0.5256 (6)	4.7 (2)
C(12)	0.4526 (3)	0.1710 (7)	0.4598 (5)	3.9 (2)
C(13)	0.4362 (3)	0.4076 (6)	0.3104 (5)	3.2 (2)
C(14)	0.3787 (4)	0.4143 (7)	0.2831 (5)	4.4 (2)
C(15)	0.3517 (5)	0.5026 (8)	0.2597 (6)	5.5 (3)
C(16)	0.3828 (5)	0.5804 (8)	0.2618 (7)	6.9 (3)
C(17)	0.4411 (5)	0.5767 (7)	0.2900 (8)	7.0 (4)
C(18)	0.4680 (4)	0.4869 (6)	0.3130 (6)	4.9 (3)
C(19)	0.3245 (3)	0.0485 (6)	0.1179 (5)	3.7 (2)
C(20)	0.3277 (4)	0.0837 (7)	0.0458 (5)	4.2 (2)
C(21)	0.2944 (4)	0.0440 (9)	−0.0326 (6)	5.7 (3)
C(22)	0.2587 (5)	−0.0317 (8)	−0.0374 (7)	6.5 (3)
C(23)	0.2542 (5)	−0.0626 (8)	0.0359 (7)	7.2 (4)
C(24)	0.2868 (5)	−0.0221 (8)	0.1141 (7)	7.0 (3)
C(25)	0.3859 (3)	−0.0067 (6)	0.2835 (5)	3.4 (2)
C(26)	0.4137 (4)	−0.0721 (6)	0.2533 (6)	3.8 (2)
C(27)	0.4339 (4)	−0.1566 (7)	0.2963 (6)	4.3 (2)
C(28)	0.4264 (4)	−0.1748 (7)	0.3696 (5)	4.0 (2)
C(29)	0.4017 (4)	−0.1131 (7)	0.4025 (6)	4.6 (2)
C(30)	0.3788 (4)	−0.0251 (7)	0.3581 (5)	4.2 (2)
C(31)	0.3095 (3)	0.1601 (6)	0.2438 (6)	3.4 (2)
C(32)	0.3171 (4)	0.1867 (7)	0.3242 (6)	4.6 (2)
C(33)	0.2744 (4)	0.2366 (8)	0.3381 (8)	5.9 (3)
C(34)	0.2255 (4)	0.2600 (8)	0.2701 (7)	5.7 (3)
C(35)	0.2189 (4)	0.2333 (9)	0.1899 (7)	6.4 (3)
C(36)	0.2611 (4)	0.1855 (7)	0.1768 (6)	4.8 (2)

[a] Anisotropically refined atoms are given in the form of the isotropic-equivalent displacement parameter defined as $^4/_3[a^2\beta_{11} + b^2\beta_{22} + c^2\beta_{33} + ab(\cos\gamma)\beta_{12} + ac(\cos\beta)\beta_{13} + bc(\cos\alpha)\beta_{23}]$.

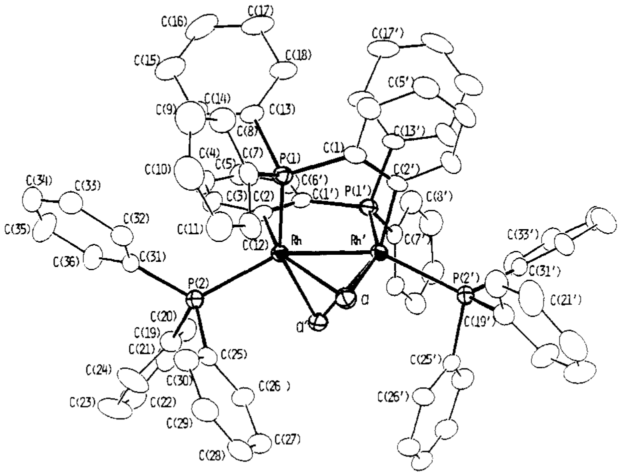

Figure 1. ORTEP drawing of the $Rh_2(\mu\text{-}Cl)_2(C_6H_4PPh_2)_2(PPh_3)_2$ molecule (**1**) showing the atom numbering. Atoms are represented as their ellipsoids of thermal displacement at the 30% probability level.

Physical Measurements. Infrared spectra were recorded by using Nujol mulls between CsI plates on a Perkin-Elmer 783 spectrophotometer. The electronic spectra were measured in dichloromethane solutions (HPLC grade) with a Cary 17D spectrophotometer. Electrochemical

---

(6) North, A. C. T.; Phillips, D. C.; Mathews, F. S. *Acta Crystallogr. Sect. A: Cryst. Phys., Diffr., Theor. Gen. Crystallogr.* **1986**, *A24*, 351.

Table III. Atomic Positional Parameters and Equivalent Isotropic Displacement Parameters (Å^2) and Their Estimated Standard Deviations for $Rh_2Cl_2(Ph_2P\{C_6H_4\})_2(PMe_3)_2$[a]

atom	*x*	*y*	*z*	*B*
Rh(1)	0.14904 (4)	0.19716 (5)	0.64843 (4)	2.37 (2)
Rh(2)	0.07725 (4)	0.21742 (5)	0.56361 (4)	2.44 (2)
Cl(1)	0.0361 (2)	0.2076 (2)	0.6659 (1)	3.24 (7)
Cl(2)	0.1089 (2)	0.0945 (2)	0.5901 (2)	3.41 (8)
P(1)	0.1559 (2)	0.3136 (2)	0.6570 (1)	2.59 (7)
P(2)	0.1573 (2)	0.2254 (2)	0.5037 (2)	2.80 (7)
P(3)	0.1815 (2)	0.1508 (2)	0.7408 (2)	3.28 (8)
P(4)	−0.0080 (2)	0.1905 (2)	0.5052 (2)	3.95 (9)
C(1)	0.0965 (6)	0.3580 (6)	0.6156 (6)	2.9 (3)
C(2)	0.0642 (6)	0.3210 (7)	0.5712 (6)	3.0 (3)
C(3)	0.0191 (6)	0.3594 (7)	0.5397 (6)	3.3 (3)
C(4)	0.0063 (7)	0.4306 (8)	0.5545 (7)	4.1 (4)
C(5)	0.0368 (7)	0.4654 (7)	0.5996 (7)	4.3 (4)
C(6)	0.0826 (7)	0.4298 (7)	0.6311 (7)	4.1 (4)
C(7)	0.2264 (6)	0.3575 (6)	0.6356 (6)	2.9 (3)
C(8)	0.2807 (6)	0.3264 (7)	0.6544 (6)	3.7 (3)
C(9)	0.3360 (7)	0.3619 (8)	0.6464 (7)	4.6 (4)
C(10)	0.3367 (8)	0.4279 (9)	0.6159 (8)	5.2 (5)
C(11)	0.2833 (8)	0.4565 (8)	0.5957 (7)	5.0 (4)
C(12)	0.2262 (7)	0.4219 (7)	0.6049 (6)	3.9 (4)
C(13)	0.1457 (6)	0.3454 (7)	0.7337 (6)	3.0 (3)
C(14)	0.1923 (7)	0.3763 (8)	0.7650 (7)	4.5 (4)
C(15)	0.1836 (8)	0.3963 (9)	0.8265 (7)	5.4 (5)
C(16)	0.1285 (7)	0.3863 (9)	0.8530 (6)	4.7 (4)
C(17)	0.0806 (8)	0.3553 (8)	0.8217 (7)	5.2 (4)
C(18)	0.0903 (7)	0.3348 (8)	0.7617 (6)	4.2 (4)
C(19)	0.2250 (6)	0.1874 (7)	0.5383 (5)	2.8 (3)
C(20)	0.2259 (6)	0.1823 (6)	0.6009 (6)	3.0 (3)
C(21)	0.2789 (6)	0.1539 (7)	0.6256 (6)	3.6 (3)
C(22)	0.3273 (4)	0.1281 (5)	0.5896 (5)	4.8 (2)
C(23)	0.3232 (4)	0.1313 (5)	0.5284 (4)	4.8 (3)
C(24)	0.2719 (4)	0.1619 (5)	0.5027 (4)	4.0 (2)
C(25)	0.1836 (4)	0.3112 (4)	0.4771 (3)	3.4 (2)
C(26)	0.1394 (5)	0.3580 (5)	0.4544 (4)	4.9 (2)
C(27)	0.1590 (6)	0.4247 (6)	0.4322 (5)	6.2 (3)
C(28)	0.2212 (7)	0.4425 (6)	0.4345 (5)	6.9 (4)
C(29)	0.2634 (5)	0.3967 (6)	0.4569 (5)	5.7 (3)
C(30)	0.2442 (4)	0.3315 (5)	0.4790 (4)	4.4 (2)
C(31)	0.1514 (4)	0.1759 (5)	0.4334 (3)	3.4 (2)
C(32)	0.1547 (4)	0.2080 (5)	0.3781 (4)	4.5 (2)
C(33)	0.1475 (4)	0.1670 (6)	0.3268 (4)	5.2 (3)
C(34)	0.1376 (5)	0.0956 (7)	0.3309 (5)	6.0 (3)
C(35)	0.1355 (5)	0.0612 (6)	0.3862 (5)	5.7 (3)
C(36)	0.1425 (5)	0.1021 (5)	0.4377 (4)	4.9 (3)
C(37)	−0.0812 (4)	0.2151 (6)	0.5389 (5)	6.0 (3)
C(38)	−0.0162 (5)	0.0933 (5)	0.4949 (6)	7.5 (4)
C(39)	−0.0169 (5)	0.2231 (7)	0.4281 (4)	6.4 (3)
C(40)	0.2447 (5)	0.1903 (5)	0.7834 (4)	5.7 (3)
C(41)	0.1226 (5)	0.1520 (6)	0.7978 (4)	5.9 (3)
C(42)	0.2018 (5)	0.0558 (5)	0.7401 (5)	5.6 (3)
C(43)	0.5 (2)	0.308 (1)	0.7 (2)	12.0 (7)*
C(44)	0.5 (2)	0.3918 (8)	0.8 (2)	5.5 (3)*
C(45)	0.4857 (6)	0.4299 (7)	0.6973 (6)	7.6 (3)*
C(46)	0.4871 (6)	0.5056 (6)	0.6993 (6)	8.4 (3)*
C(47)	0.5 (2)	0.537 (1)	0.8 (2)	9.9 (6)*
O	0.5 (2)	0.042 (1)	0.8 (2)	19.7 (8)*
C(48)	0.569 (2)	0.051 (2)	0.735 (2)	11 (1)*
C49)	0.603 (2)	0.091 (3)	0.730 (2)	13 (1)*
C(50)	0.515 (2)	0.137 (2)	0.790 (2)	11.6 (9)*
C(51)	0.435 (3)	0.109 (4)	0.763 (3)	20 (3)*

[a] Starred values are for atoms refined isotropically. Anisotropically refined atoms are given in the form of the equivalent isotropic displacement parameter defined as $^4/_3[a^2\beta_{11} + b^2\beta_{22} + c^2\beta_{33} + ab(\cos\gamma)\beta_{12} + ac(\cos\beta)\beta_{13} + bc(\cos\alpha)\beta_{23}]$.

measurements were performed with a Bioanalytical Systems, Inc., Model BAS 100 electrochemical analyzer in conjunction with a Houston Instruments Model DMP 40 digital plotter. Experiments were carried out in dichloromethane solutions that were 0.2 M in tetra-*n*-butylammonium hexafluorophosphate (TBAH) as a supporting electrolyte. A three-electrode cell configuration was used, with a platinum disk (Model BAS MF 2032) and a platinum wire as working and auxiliary electrodes, respectively. A BAS MF 2020 Ag/AgCl reference electrode was employed (−35 mV vs SCE).

Results and Discussion

Synthetic Methods. Complexes **1** and **2** were prepared from $Rh_2(O_2CCH_3)_2(C_6H_4PPh_2)_2{\cdot}2CH_3COOH$. The acetate groups were replaced by Cl by the action of Me_3SiCl in warmed THF solutions of the starting material. The addition of monodentate phosphines after the chlorination of the dirhodium starting material afforded **1** and **2** in high yields. $Rh_2(O_2CCH_3)_2(C_6H_4PPh_2)_2{\cdot}2CH_3COOH$ forms an adduct upon the addition of THF, as indicated by a color change from purple to blue. The subsequent addition of 4 equiv of Me_3SiCl to warmed solutions of the THF adduct caused the color of the solution to change to dark green, indicating the formation of an intermediate of the type $Rh_2Cl_2(C_6H_4PPh_2)_2{\cdot}2THF$. To this solution was added 2 equiv of the monodentate phosphine, causing an immediate color change from dark green to dark red. Within 10 min, the color of the solution intensified to a bright orange-red. The same products are obtained regardless of whether the reaction is worked up after 10 min or after 24 h of reflux, nor does the addition of excess monodentate phosphine (up to 6 equiv) change the result.

It is instructive to compare the preparative reaction for the present compounds (eq 1) with that for $Rh_2Cl_2(dmpm)_2(C_6H_4PPh_2)_2$[1] (eq 2). Even when 4 equiv of PR_3 is used, the same

$$Rh_2(O_2CCH_3)_2(C_6H_4PPh_2)_2 \xrightarrow{2Me_3SiCl\ +\ 2PR_3} Rh_2(\mu\text{-}Cl)_2(C_6H_4PPh_2)_2(PR_3)_2 \quad (1)$$

$$Rh_2(O_2CCH_3)_2(C_6H_4PPh_2)_2 \xrightarrow{2Me_3SiCl\ +\ 2dmpm} Rh_2Cl_2(C_6H_4PPh_2)_2(dmpm)_2 \quad (2)$$

product, which contains μ-Cl atoms and only two PR_3 ligands, is obtained. It is apparently necessary to have pairs of P atoms united by the methylene groups in dmpm to overcome a strong tendency of the Cl atoms to take up bridging positions, which they also do in $Rh_2Cl_4(dppm)_2$.

Physical Properties. The two compounds have broadly similar electronic spectra. The band positions, with λ_{max} in nanometers and ϵ values in parentheses, are as follows: **1**, 325 (sh), 375 (sh), 420 (15750), 480 (sh); **2**, 330 (sh), 430 (4200).

For each compound, the cyclic voltammetry shows two oxidation processes. For **1** the processes, at +0.747 and +1.077 V, were coupled with reductions on the reverse sweep. The peak separations of 72 and 61 mV together with the virtually equal peak current values suggest that we are observing two reversible (or nearly reversible) one-electron oxidations of **1**. No reduction was seen out to −1.2 V. For **2** there were also two oxidations and no reduction (out to −1.6 V), but the oxidations are clearly irreversible. An oxidation wave at +0.534 V was separated by 90 mV from the reverse reduction, and the $i_{p,c}/i_{p,a}$ ratio was about 2. For the second oxidation, at +1.008 V, no reverse reduction was recorded. In one or both cases we may be dealing with coupled reactions.[7,8]

Structural Results. The structures of compounds **1** and **2** are shown in Figures 1 and 2, respectively. In each case the molecule is chiral, with either rigorous (**1**) or effective (**2**) C_2 symmetry. The $C_6H_4PPh_2$ ligands retain the cisoid, head-to-tail relationship that they had in the starting material. The molecules are generally similar, with Rh–Rh bond lengths of 2.499 (1) and 2.506 (1) Å, respectively, which may be compared with the value in the similarly structured molecules $Rh_2Cl_4(dppm)_2$ of 2.523 (2) Å.

Molecules of **1** and **2** differ, however, in several respects. The Rh–P distances to the terminal phosphine ligands are somewhat different, with a value of 2.403 (2) Å in **1** and two slightly different but shorter values, 2.363 (4) and 2.348 (4) Å, in **2**. The shorter distances in **2** are of course consistent with the facts that PMe_3 is more basic as well as less sterically demanding than PPh_3, although the greater π-acidity of the latter might tend to offset these factors. There is also a significant difference in the degree of twisting of the orthometalated ligands in the two compounds.

---

(7) Adams, R. N. *Electrochemistry at Solid Electrodes*; Marcel Dekker: New York, 1969.

(8) Nicholson, R. S.; Shain, I. *Anal. Chem.* **1964**, *36*, 706.

Table IV. Selected Bond Distances and Bond Angles for $Rh_2Cl_2(Ph_2P\{C_6H_4\})_2(PPh_3)_2$[a]

		Bond Distances (Å)			
Rh–Rh′	2.499 (1)	Rh–C(2)	2.021 (8)	P(2)–C(25)	1.835 (9)
Rh–Cl	2.570 (2)	P(1)–C(1)	1.820 (8)	P(2)–C(31)	1.838 (10)
Rh–Cl′	2.425 (2)	P(1)–C(7)	1.861 (10)	C(1)–C(2′)	1.425 (14)
Rh–P(1)	2.234 (2)	P(1)–C(13)	1.824 (8)	C(1)–C(6)	1.396 (11)
Rh–P(2)	2.403 (2)	P(2)–C(19)	1.848 (8)	C(7)–C(12)	1.395 (13)
		Bond Angles (deg)			
Rh′–Rh–Cl	57.14 (6)	Cl′–Rh–P(1)	153.78 (8)	Rh–P(2)–C(19)	118.3 (4)
Rh′–Rh–Cl′	62.92 (5)	Cl′–Rh–P(2)	96.63 (8)	C(19)–P(2)–C(25)	98.4 (4)
Rh′–Rh–P(1)	90.93 (6)	Cl′–Rh–C(2)	89.1 (3)	P(1)–C(1)–C(2′)	120.1 (5)
Rh′–Rh–P(2)	152.40 (6)	P(1)–Rh–P(2)	108.67 (9)	C(2′)–C(1)–C(6)	120.5 (7)
Rh′–Rh–C(2)	97.8 (3)	P(1)–Rh–C(2)	93.0 (2)	Rh–C(2)–C(1′)	120.3 (6)
Cl–Rh–Cl′	80.81 (7)	P(2)–Rh–C(2)	100.3 (2)	P(1)–C(7)–C(12)	118.1 (7)
Cl–Rh–P(1)	86.48 (7)	Rh–Cl–Rh′	59.94 (5)	C(8)–C(7)–C(12)	123.0 (9)
Cl–Rh–P(2)	103.65 (7)	Rh–P(1)–C(1)	109.9 (3)	P(2)–C(19)–C(20)	120.8 (7)
Cl–Rh–C(2)	154.9 (3)	C(1)–P(1)–C(7)	104.3 (4)	C(20)–C(19)–C(24)	120.9 (8)

[a] Numbers in parentheses are estimated standard deviations in the least significant digits.

Table V. Selected Bond Distances and Bond Angles for $Rh_2Cl_2(Ph_2P\{C_6H_4\})_2(PMe_3)_2$

		Bond Distances (Å)			
Rh(1)–Rh(2)	2.506 (1)	Rh(2)–Cl(2)	2.503 (3)	P(3)–C(40)	1.850 (11)
Rh(1)–Cl(1)	2.529 (3)	Rh(2)–P(2)	2.224 (3)	P(3)–C(41)	1.823 (11)
Rh(1)–Cl(2)	2.506 (3)	Rh(2)–P(4)	2.348 (4)	P(3)–C(42)	1.855 (10)
Rh(1)–P(1)	2.220 (3)	Rh(2)–C(2)	1.991 (13)	C(1)–C(2)	1.41 (2)
Rh(1)–P(3)	2.363 (4)	P(1)–C(1)	1.815 (13)	C(1)–C(6)	1.44 (2)
Rh(1)–C(20)	2.023 (13)	P(1)–C(7)	1.828 (13)		
Rh(2)–Cl(1)	2.477 (3)	P(1)–C(13)	1.838 (13)		
		Bond Angles (deg)			
Rh(2)–Rh(1)–Cl(1)	58.92 (8)	Cl(2)–Rh(1)–P(3)	106.1 (1)	Rh(1)–P(3)–C(40)	122.2 (4)
Rh(2)–Rh(1)–Cl(2)	59.92 (8)	Cl(2)–Rh(1)–C(20)	85.0 (4)	C(40)–P(3)–C(41)	99.7 (5)
Rh(2)–Rh(1)–P(1)	87.55 (9)	P(1)–Rh(1)–P(3)	105.8 (1)	P(1)–C(1)–C(2)	119.8 (9)
Rh(2)–Rh(1)–P(3)	156.2 (1)	P(1)–Rh(1)–C(20)	97.3 (4)	P(1)–C(1)–C(6)	118 (1)
Rh(2)–Rh(1)–C(20)	98.6 (4)	P(3)–Rh(1)–C(20)	99.1 (4)	C(2)–C(1)–C(6)	122 (1)
Cl(1)–Rh(1)–Cl(2)	78.1 (1)	Rh(1)–Rh(2)–Cl(1)	61.00 (8)	Rh(2)–C(2)–C(1)	118.4 (9)
Cl(1)–Rh(1)–P(1)	88.6 (1)	Cl(1)–Rh(2)–Cl(2)	79.1 (1)	Rh(1)–C(20)–C(19)	120.4 (9)
Cl(1)–Rh(1)–P(3)	101.0 (1)	Rh(1)–Cl(1)–Rh(2)	60.08 (8)	C(19)–C(20)–C(21)	116 (1)
Cl(1)–Rh(1)–C(20)	156.6 (4)	Rh(1)–P(1)–C(1)	111.5 (4)		
Cl(2)–Rh(1)–P(1)	147.3 (1)	C(1)–P(1)–C(7)	105.5 (6)		

[a] Numbers in parentheses are estimated standard deviations in the least significant digits.

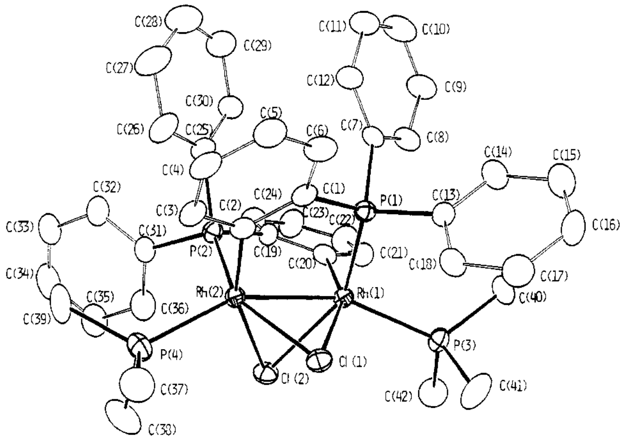

Figure 2. ORTEP drawing of the $Rh_2(\mu\text{-}Cl)_2(C_6H_4PPh_2)_2(PMe_3)_2$ molecule (**2**) showing the atom numbering. Each atom is represented by its ellipsoid of thermal displacement at the 30% probability level.

The C–Rh–Rh–P torsion angles are 0.29° in **1** and 10.7° in **2**.

Despite the moderate torsional twist in **2** it may still be said that both molecules consist of square pyramidally coordinated Rh atoms sharing a common basal edge (Cl···Cl) and having the monodentate phosphine atoms at the apex. The Rh–Rh–P angles are essentially the same (ca. 153°) in the two molecules.

It is noteworthy that once again this type of structure, with two μ-Cl groups, has been adopted. The possibility certainly exists, at least for the small PMe_3 ligand, that two more phosphine ligands might have been incorporated so as to give a structure like that of $Rh_2(C_6H_4PPh_2)_2(dmpm)_2Cl_2$. In this type of structure, as in the one actually adopted, there would be a total of 10 metal–ligand bonds as well as a Rh–Rh bond. Evidently, the two types of structures do not differ greatly in stability and small, largely unpredictable factors can determine the preference in any given case.

Acknowledgment. We thank the National Science Foundation for support and Drs. Rinaldo Poli, Lee Daniels, and L. R. Falvello for crystallographic advice.

Registry No. **1**, 110745-24-9; **2**, 110745-26-1; $Rh_2(O_2CCH_3)_2(C_6H_4PPh_2)_2$, 92669-59-5; Rh, 7440-16-6; $Rh_2Cl_2(C_6H_4PPh_2)_2(PMe_3)_2$, 110745-25-0.

Supplementary Material Available: For the crystal structures of **1** and **2**, full tables of bond distances, bond angles, and anisotropic displacement parameters (15 pages); tables of observed and calculated structure factors (56 pages). Ordering information is given on any current masthead page.

Contribution from the Department of Chemistry
and Laboratory for Molecular Structure and Bonding,
Texas A&M University, College Station, Texas 77843

Two Diastereomeric Forms of the Bischelated, Edge-Sharing Bioctahedral Molecule $Ta_2Cl_6(Et_2PCH_2CH_2PEt_2)_2$

F. Albert Cotton,* Michael P. Diebold, and Wieslaw J. Roth

Received June 3, 1987

Chelate rings in metal complexes can often exist in more than one conformation. Five membered nonplanar rings such as those formed by chelating depe (depe = bis(diethylphosphino)ethane)